AGU PUBLICATIONS

JGR

Journal of Geophysical Research: Atmospheres

RESEARCH ARTICLE
10.1002/2015JD023267

Key Points:
- Nitrous oxide lifetime is computed empirically from MLS satellite data
- Empirical N_2O lifetimes compared with models including interannual variability
- Results improve values for present anthropogenic and preindustrial emissions

Correspondence to:
M. J. Prather,
mprather@uci.edu

Citation:
Prather, M. J., et al. (2015), Measuring and modeling the lifetime of nitrous oxide including its variability, *J. Geophys. Res. Atmos.*, *120*, 5693–5705, doi:10.1002/2015JD023267.

Received 18 FEB 2015
Accepted 8 MAY 2015
Accepted article online 14 MAY 2015
Published online 5 JUN 2015

©2015. The Authors.
This is an open access article under the terms of the Creative Commons Attribution-NonCommercial-NoDerivs License, which permits use and distribution in any medium, provided the original work is properly cited, the use is non-commercial and no modifications or adaptations are made.

Measuring and modeling the lifetime of nitrous oxide including its variability

Michael J. Prather[1], Juno Hsu[1], Nicole M. DeLuca[1], Charles H. Jackman[2], Luke D. Oman[2], Anne R. Douglass[2], Eric L. Fleming[2,3], Susan E. Strahan[3], Stephen D. Steenrod[2,4], O. Amund Søvde[5], Ivar S. A. Isaksen[6], Lucien Froidevaux[7], and Bernd Funke[8]

[1]Earth System Science, University of California Irvine, Irvine, California, USA, [2]NASA Goddard Space Flight Center, Greenbelt, Maryland, USA, [3]Science Systems and Applications, Inc., Lanham, Maryland, USA, [4]Goddard Earth Sciences Technology and Research Center, Universities Space Research Association, Columbia, Maryland, USA, [5]Center for International Climate and Environmental Research–Oslo, Oslo, Norway, [6]Department of Geosciences, University of Oslo, Oslo, Norway, [7]Jet Propulsion Laboratory, Pasadena, California, USA, [8]Instituto de Astrofísica de Andalucía, CSIC, Granada, Spain

Abstract The lifetime of nitrous oxide, the third-most-important human-emitted greenhouse gas, is based to date primarily on model studies or scaling to other gases. This work calculates a semiempirical lifetime based on Microwave Limb Sounder satellite measurements of stratospheric profiles of nitrous oxide, ozone, and temperature; laboratory cross-section data for ozone and molecular oxygen plus kinetics for $O(^1D)$; the observed solar spectrum; and a simple radiative transfer model. The result is 116 ± 9 years. The observed monthly-to-biennial variations in lifetime and tropical abundance are well matched by four independent chemistry-transport models driven by reanalysis meteorological fields for the period of observation (2005–2010), but all these models overestimate the lifetime due to lower abundances in the critical loss region near 32 km in the tropics. These models plus a chemistry-climate model agree on the nitrous oxide feedback factor on its own lifetime of 0.94 ± 0.01, giving N_2O perturbations an effective residence time of 109 years. Combining this new empirical lifetime with model estimates of residence time and preindustrial lifetime (123 years) adjusts our best estimates of the human-natural balance of emissions today and improves the accuracy of projected nitrous oxide increases over this century.

1. Introduction

Nitrous oxide (N_2O) is the third-most-important, long-lived greenhouse gas, after carbon dioxide and methane [*Myhre et al.*, 2013]. These top-three greenhouse gases have a mixture of natural and anthropogenic sources, and the challenge has always been to quantify the human perturbation to their budgets [*Prather et al.*, 2012; *Ciais et al.*, 2013]. Surface emissions of N_2O have an average atmospheric residence time of a century or more [*Ko et al.*, 1991; *World Meteorological Organization* (*WMO*), 2014], and thus, the current imbalance between emissions and atmospheric loss, as quantified by the observed growth rate of 3.8 Tg N/yr (0.8 ppb/yr), is expected to lead to further increases in N_2O abundances over this century, even if anthropogenic emissions are stabilized.

Anthropogenic emissions of N_2O are driven primarily by fertilizer use and the handling of animal wastes, sources difficult both to control and to quantify [*Galloway et al.*, 2008; *Erisman et al.*, 2013]. Estimates of N_2O emissions from summing individual sources have greater than factor of 2 uncertainties [*Prather et al.*, 2009; *Ciais et al.*, 2013], and atmospheric inversions rely on the accuracy of stratospheric losses and emission patterns [*Thompson et al.*, 2014]. Scenarios for future N_2O levels make assumptions about both present-day and preindustrial N_2O lifetimes to determine the anthropogenic-natural balance in emissions levels [*Meinshausen et al.*, 2011; *Kirtman et al.*, 2013]. Thus, the uncertainties in the current budget and 21st century projections of N_2O are its lifetime and the feedback that an N_2O perturbation has on its lifetime [*Prather*, 1998]. Assessment of the lifetime and feedback has been notably absent from climate and ozone assessments [*Intergovernmental Panel on Climate Change (IPCC)*, 2007; *WMO*, 2011; *IPCC*, 2013a] but has received more attention in the past couple years [*Stratospheric Processes and their Role in Climate* (*SPARC*), 2013; *Chipperfield et al.*, 2014; *WMO*, 2014].

In this paper we combine satellite measurements of N_2O, O_3, and temperature (T) from the Aura Microwave Limb Sounder (MLS) instrument [*Lambert et al.*, 2007; *Froidevaux et al.*, 2008; *Schwartz et al.*, 2008] with global

chemistry models to derive a semiempirical (measured) lifetime for N_2O. Previous studies have been done with less extensive satellite data [*Ko et al.*, 1991; *Minschwaner et al.*, 1998, 2013]. This lifetime is constrained by the observation of all quantities controlling N_2O loss, is independent of transport uncertainties, and includes seasonal and year-to-year variability. The only chemical modeling involves photolysis rates for N_2O and O_3 and the kinetics of the $O(^1D)$ reactions. Uncertainties in this semiempirical lifetime are due only to possible errors in these chemical rates and in the measured profiles of N_2O, O_3, and T in the critical region (3–30 hPa in the tropics).

Four chemistry-transport models (CTMs) using meteorological data for the Aura period are compared with monthly MLS observations of stratospheric N_2O and O_3, the N_2O losses derived therefrom, and stratospheric NO_y from the Environmental Satellite Michelson Interferometer for Passive Atmospheric Sounding (MIPAS) [*Funke et al.*, 2014] in order to understand the cause of model errors in N_2O lifetime. In addition, two chemistry-climate models (CCMs, one 3-D and one 2-D) with climate-driven circulations are also evaluated against the average MLS-derived lifetime. The models evaluated here overestimate the semiempirical lifetime, 116 ± 9 years, by a wide range, but agree on the negative sensitivity of lifetime to burden of -0.065 ± 0.010 (not constrained by observations) that results in a lower residence time for N_2O perturbations of 109 years. A best estimate for preindustrial conditions gives a longer lifetime of 123 years due primarily to reduced photochemical rates for N_2O loss because of increased midstratospheric and upper stratospheric O_3 caused by reduced levels of chlorine and N_2O.

Results from the MLS data and the constrained photochemical models are described in section 2. The CTMs, their calculation of N_2O lifetimes, and their comparison with stratospheric constituents and the constrained N_2O loss are presented in section 3. In section 4, four models are used to estimate the reduction in lifetime when N_2O increases and the change in lifetime since the preindustrial era. An overview of issues related to N_2O lifetime is discussed in section 5.

2. N_2O Lifetime Derived From MLS Observations

The MLS instrument on the NASA Aura satellite provides highly accurate, well-resolved latitude-by-altitude co-located profiles of N_2O, O_3, and T throughout the stratosphere [*Lambert et al.*, 2007; *Livesey et al.*, 2011; *Schwartz et al.*, 2008]. Here we use monthly mean MLS data sets from August 2004 to December 2010 (version 2.2 for O_3 and version 3.3 for N_2O and T). Profiles are averaged longitudinally and within 5° latitude bins from 85°S–80°S to 80°N–85°N (34 in total; MLS observations are limited to 82°S–82°N). For global budgets, the 80°–85° latitude bins were extended to 90°. There are six standard pressure levels per decade in pressure (i.e., 100, 68, 46, 32, 22, 15, 10, up to 0.10 hPa). These data sets are very similar to the monthly mean data records produced for the Global OZone Chemistry And Related trace gas Data records for the Stratosphere project [*Froidevaux et al.*, 2015].

The vertical profiles of O_3 and T define all the conditions needed to calculate the profiles of N_2O loss and NO_y production from the following reactions ((R1)–(R5)). The rates of these reactions respond primarily to overhead O_3 column and T.

(R1) $$O_3 + h\nu \Rightarrow O(^1D) + O_2$$

(R2) $$O(^1D) + (N_2, O_2) \Rightarrow O + (N_2, O_2)$$

(R3) $$N_2O + h\nu \Rightarrow N_2 + O(^1D)$$

(R4) $$N_2O + O(^1D) \Rightarrow N_2 + O_2$$

(R5) $$N_2O + O(^1D) \Rightarrow NO + NO$$

We use two independent photochemical submodels, one from NASA Goddard Space Flight Center (GSFC, embedded in the G2d model) and one from University of California, Irvine (embedded in the UCI CTM; see Table 1). These submodels solve the 1-D radiative transfer problem to calculate J-N_2O (reaction (R3)) and O (^1D) densities (reactions ((R1) and (R2)) and are documented in photolysis studies [*Olson et al.*, 1997; *PhotoComp*, 2010]. While the methodologies and numerical approaches for both are independent, they (and all the chemistry-transport models here) adopt standard values for the cross sections (O_2, O_3, and N_2O) and rate coefficients controlling these reactions [*Sander et al.*, 2011]. The UCI version (MLS-U) uses

Table 1. Measurements and Models

Name	Type	Core Elements	Meteorological Data	Period	References
MLS	measured	N_2O, O_3, and T		Aug 2004/2010	*Lambert et al.* [2007], *Froidevaux et al.* [2008], and *Schwartz et al.* [2008]
MIPAS	measured	NO_y		2007/2010	*Funke et al.* [2014]
MLS-G	measured + modeled	GSFC 2-D J values		2005/2010	*Fleming et al.* [2011] and *Jackman et al.* [2014]
MLS-U	measured + modeled	UCI J values		2005/2010	*Olson et al.* [1997], *Bian and Prather* [2002], and *PhotoComp* [2010]
GMI	modeled	GMI Combo CTM	MERRA GEOS-5	2004/2010	*Douglass et al.* [2004] and *Strahan et al.* [2013]
GEOSCCM	modeled	StratChem + GMAO GEOS-5 GCM	33 years of prescribed SSTs	(typical of 2000s decade)	*Li et al.* [2012] and *Oman and Douglass* [2014]
Oslo-c29	modeled	Oslo CTM3	EC IFS cycles 29/31	2004/2007	*Søvde et al.* [2012]
Oslo-c36	modeled	Oslo CTM3	EC IFS cycle 36r1	1997/2009	*Ibidem*
UCI-c29	modeled	UCI CTM	EC IFS cycles 29/31	2000/2007	*Hsu and Prather* [2010] and *Prather and Hsu* [2010]
UCI-c36	modeled	UCI CTM	EC IFS cycle 36r1	1997/2010	*Ibidem*
G2d-M	modeled	GSFC 2-D, specified transport	MERRA GEOS-5	1979/2010	*Fleming et al.* [2011] and *Jackman et al.* [2014]
G2d	modeled	GSFC 2-D, interactive transport	Steady state yearly repeating	(typical of 2010)	*Ibidem*

the standard MLS levels (2.7 km) and integrates monthly, latitude-resolved losses from 0.10 hPa to 100 hPa. The GSFC version (MLS-G) interpolates and fills the MLS data and integrates at 1 km resolution through the atmosphere. Given the linear N_2O profile in the dominant loss region (Figures 1a and 2a), the integrated loss should not be sensitive to interpolation methods. From MLS-G we find that about 2% of N_2O loss occurs at altitudes below 100 hPa. From previous studies with the UCI CTM [*Prather and Hsu*, 2010] we found that 1% of N_2O loss occurs through reaction with $O(^1D)$ in the troposphere. Thus, N_2O losses from MLS-U are corrected upward by 2%, and those from the UCI CTM (running here without tropospheric chemistry) are corrected upward by 1%.

The critical region for N_2O loss is the tropical middle stratosphere as shown in Figures 1a and 1b. Photochemical loss (dominated by R3) peaks at the equator near 32 km pressure altitude. Both models MLS-G and MLS-U agree on the integrated loss averaged over years 2005–2010, although coarse vertical layering for MLS-U (vertical black bars) obscures the peak loss. In terms of total loss, 81% occurs between 24 and 40 km including all latitudes, while 76% occurs between 30°S and 30°N including all heights. Polar regions produce only 4% of the loss, and that occurs at high altitudes, so that ozone depletion below 24 km has minimal direct photochemical impact on the N_2O lifetime. This evaluation does not include possible circulation changes. Ozone depletion from the ClO catalytic cycle (40–50 km altitudes) does impact the N_2O lifetime: see discussion of preindustrial lifetime (section 4). Figure 2a shows the vertical profile of MLS N_2O from 16 to 48 km in pressure altitude averaged over 30°S to 30°N for years 2005–2010, and Figure 2b, that of MLS O_3. Note that the peak loss (Figure 1a) centers on the 50% (~160 ppb) level of N_2O at about 10 hPa (32 km). The critical region for modeling the N_2O lifetime thus centers on the region 30°S–30°N and 24 km to 40 km. The MLS observations show that monthly zonal-mean N_2O abundances at 10 hPa have large seasonal and interannual variations (Figure 3a). The upwelling region with highest N_2O levels, and hence greatest loss, occurs in the tropics (20°S–20°N; white lines in Figures 3a–3e), where the MLS monthly average at 10 hPa ranges from 147 to 206 ppb.

With this variability in the critical loss region, we expect large seasonal and interannual variations in the N_2O loss rate. The 5 year averaged monthly mean loss rates are shown in Figure 4 for MLS-G (black solid + dots) and MLS-U (black dashed). Not unexpectedly, both chemical submodels give nearly identical results with a mean loss rate of 13.2 Tg N/yr and peak-to-peak amplitude of 25%. The peak losses occur with the peak upwelling (January-February-March) seen in Figure 3. The interannual variation in N_2O lifetime is calculated as 12 month running averages of the burden

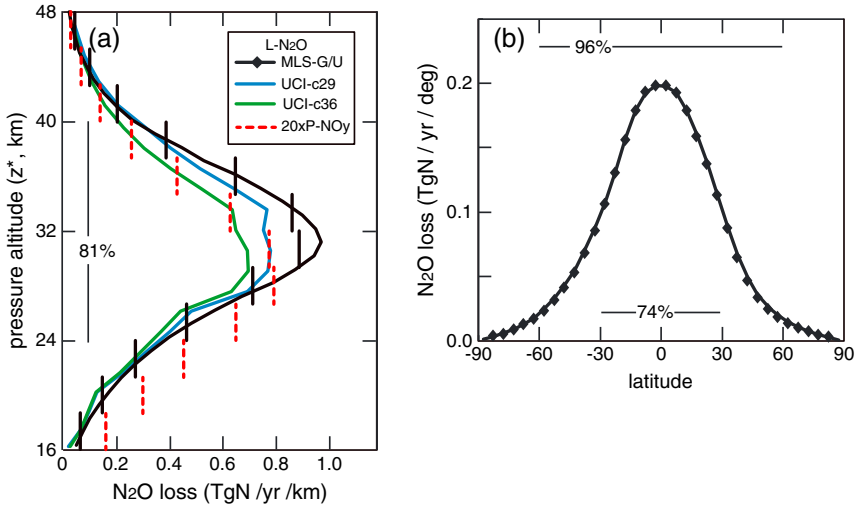

Figure 1. Multiyear annual average loss of N_2O plotted against (a) pressure altitude (z^* km, units Tg N/yr/km) and (b) latitude (degrees, units Tg N/yr/deg). Results are shown for MLS-G (black solid line) and MLS-U (black vertical bars or diamonds). MLS-U was integrated with coarser vertical resolution. Percentages indicate the fraction of total loss within the range. MLS-U primary production of NO_y (times 20) is also shown in Figure 1a (red dashed vertical bars). N_2O loss from the UCI CTM is shown for IFS cycles 29 (blue) and 36 (green).

(Tg N = 4.79 times lower tropospheric mean abundance in ppb) divided by the 12 month accumulated loss (Tg N/yr) and is plotted for MLS-G and MLS-U from 1 February 2005 to 1 July 2010 in Figure 5. The calendar mean (January–December) lifetimes for MLS-G are shown as dots. The mean burden over the MLS period is calculated as 1539 Tg N, and the mean loss is 13.2 Tg N/yr, giving a lifetime of ~116.5 years for both photochemical submodels (see Table 1). A quasi-biennial signal is clear over the 5 years of MLS data, and the minimum-to-maximum amplitude is about 10%.

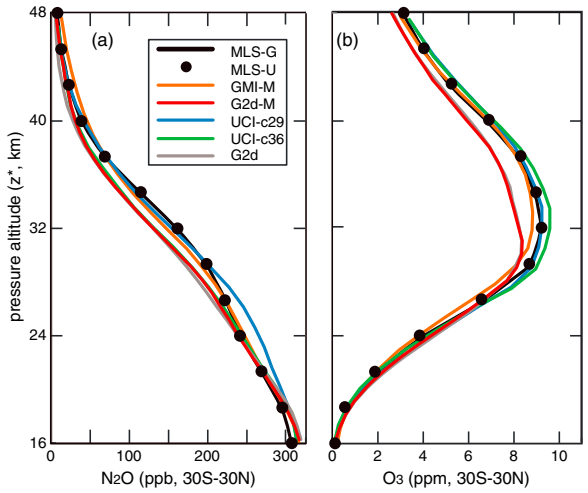

Figure 2. Tropical (30°S–30°N) profiles of (a) N_2O (ppb) and (b) O_3 (ppm) as a function of pressure altitude (z^* km) average over 2005–2010 where available. MLS-G (solid black) is interpolated to 1 km resolution, and MLS-U (black dots) shows the original MLS resolution. Also shown are the modeled profiles for GMI (orange), G2d-M (red), UCI-c29 (blue), UCI-c36 (green), and G2d (gray). Results for Oslo-c29 and Oslo-c36 are almost identical to the UCI model.

The N_2O lifetime varies with solar activity, and MLS-G and MLS-U evaluated this by changing the solar spectrum and thus the photolysis rates, which are summarized in Table 2. MLS-G has the more accurate treatment, and its 2005–2010 lifetime value uses the actual solar activity of the time period (mostly solar minimum). MLS-G then repeated the calculation using constant minimum and maximum solar activities, giving a span of 7% (109 years at solar maximum to 117 years at solar minimum). This range uses the fixed MLS observations of O_3 and T, which are more suitable to solar minimum conditions, and thus, background atmospheric changes expected at solar maximum (including the N_2O) are not included. MLS-U uses a solar spectrum that averages minimum and high (but not maximum) solar activity. Thus, the standard 2005–2010 MLS-U lifetime represents higher solar activity than occurred for the period, and the agreement with MLS-G is fortuitous since

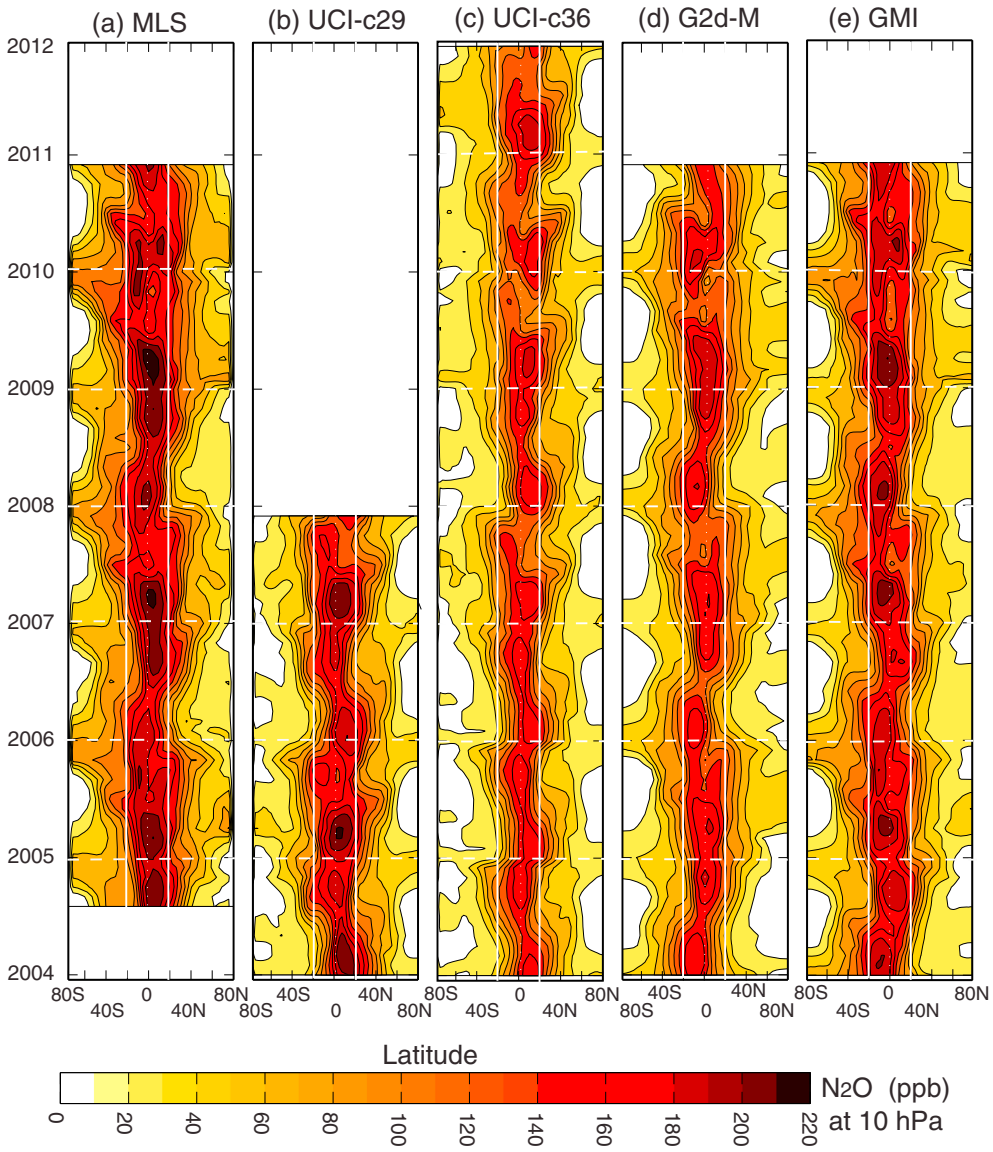

Figure 3. Contours of N_2O at 10 hPa plotted as function of latitude and month from January 2004 to December 2011. Results are shown for (a) MLS, (b) UCI-c29, (c) UCI-c36, (d) G2d-M, and (e) GMI.

the solar-minimum calculation gives a slightly longer lifetime of 119 years. Both models show a similar response to changes in the solar spectrum when the difference in minimum-maximum ranges is considered. The 2005–2010 period covers an extended solar minimum period; the solar activity of the current cycle 24 is weaker than average and expected to reach maximum in 2015 [*Pesnell*, 2014].

Combining interannual variability and other uncertainties, we derive the N_2O lifetime of 116 ± 9 years for the period of 2005–2010. Comparison with modeled values follows, and the 1 sigma uncertainty of ±8% is derived in section 4.

3. Model-Measurement Comparisons

Four CTMs used meteorological data for the MLS period and before, calculating N_2O lifetimes to compare with the MLS-G/U results. See Table 1. Two of these (NASA Global Modeling Initiative CTM (GMI) and GSFC 2-D model (G2d-M)) used the Modern-Era Retrospective Analysis for Research and Applications (MERRA) Goddard Earth

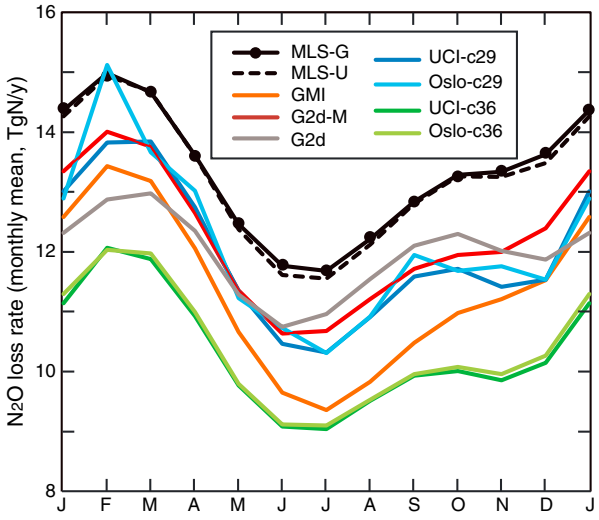

Figure 4. Monthly N_2O loss rate (units of Tg N/yr) for the MLS period of 2005–2010 or best equivalent period from MLS-G (black solid + dots), MLS-U (black dashed), GMI (orange), G2d-M (red), G2d (gray), UCI-c29 (dark blue), Oslo-c29 (light blue), UCI-c36 (dark green), and Oslo-c36 (light green).

Observing System version 5(GEOS-5) assimilation met data (designated GMI and G2d-M, respectively). The GSFC 2-D model with interactive transport (G2d) also ran a standard simulation and sensitivity studies for steady state, yearly repeating 2010 conditions. The GSFC Goddard Earth Observing System Chemistry Climate Model (GEOSCCM) is a free-running atmospheric climate model driven by prescribed sea surface temperatures. UC Irvine and University of Oslo CTMs used the European Centre for Medium-Range Weather Forecasts' (ECMWF) Integrated Forecast System (IFS) to generate pieced forecasts, and two different cycles of the IFS generated met data that partially overlap (designated UCI-c29, UCI-c36, Oslo-c29, and Oslo-c36 according to which IFS cycle was used). Model resolution was typically 2°–3° horizontally and 60–80 levels. The Oslo and UCI models used identical met data and tracer-transport models, but Oslo has full stratosphere-troposphere chemistry (like GMI), whereas UCI uses a linearized stratospheric chemistry model (O_3, N_2O, NO_y, CH_4, and H_2O [see *Hsu and Prather*, 2010]). G2d-M and G2d have full stratospheric chemistry but not detailed tropospheric chemistry.

Globally integrated N_2O loss versus altitude from UCI-c29 and UCI-c36 are compared with MLS-G/U in Figure 1a. Both UCI models match the MLS shape but calculate losses that are smaller by 10% (c29) and 20% (c36)

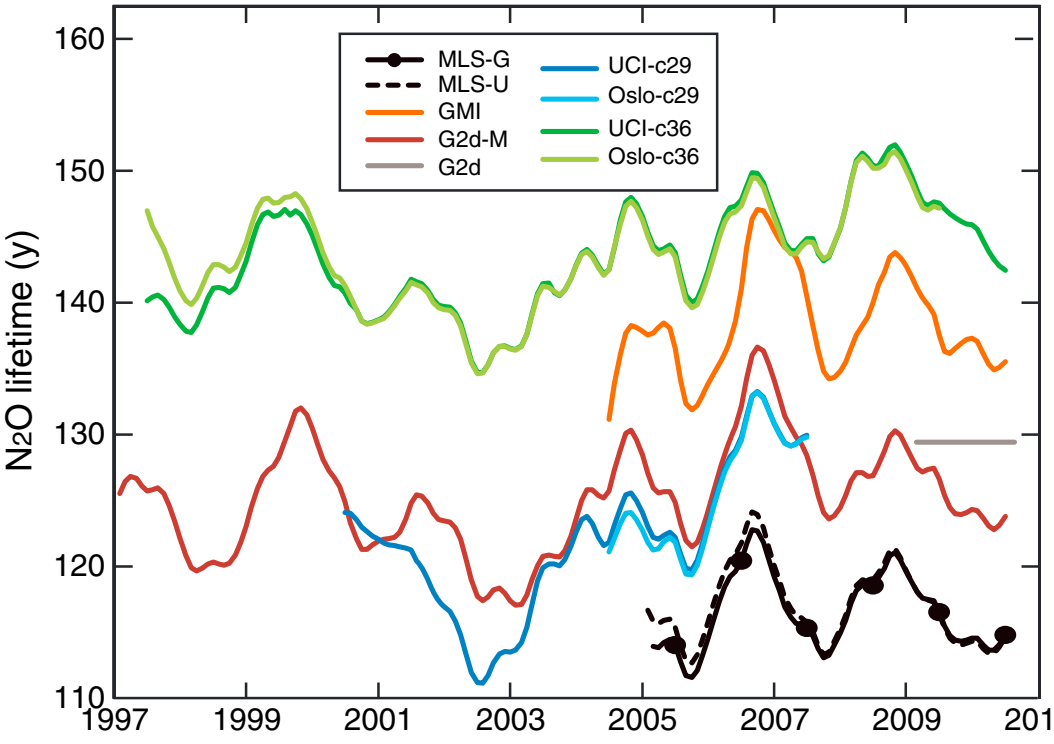

Figure 5. Annual N_2O lifetime (year) showing interannual variability. Values are derived from 12 month average burden (Tg N) and loss rate (Tg N/yr) centered on each month. For description of measurements and models shown, see Figure 4.

Table 2. Present-Day N_2O Lifetime and Other Model Comparisons[a]

	N_2O Lifetime (Year)						
	(2004/2010)	(1997/2010)	Solar Maximum	Solar Minimum	Stratospheric N_2O (ppb)	NO_y (DU)	Lifetime Sensitivity
MLS-G	116.3		108.7	116.9	176 ± 15		
MLS-U	117.1		115.1	119.2	176 ± 15		
MIPAS						0.387	
GMI	137.4				160 ± 15	0.378	
GEOSCCM	120.2				171 ± 12	0.376	−0.055
G2d-M	127.0	125.2			143 ± 16	0.418	−0.062
G2d	129.5				144 ± 5	0.431	−0.117
Oslo-c29	126.1				162 ± 20	0.339	−0.062
Oslo-c36	146.7	144.7			138 ± 14	0.389	−0.056
UCI-c29	126.2				162 ± 20	0.345	−0.078
UCI-c36	146.2	143.8			137 ± 14	0.395	−0.070
Recommended			**116 ± 9**				**−0.065 ± 0.010**

[a]Note that stratospheric N_2O is multiyear average at 10 hPa, 20°S–20°N. Stratospheric NO_y is the multiyear averaged column above 100 hPa, 30°S–30°N. The lifetime sensitivity $s \equiv \partial \ln(\text{lifetime})/\partial \ln(\text{burden})$ is related to the feedback factor as $ff = 1/(1 - s)$ [*Prather*, 2007]. Lifetimes are calculated as the annual average burden (Tg N) divided by the accumulated annual loss (Tg N/yr), and all are based on a transient N_2O burden increasing at 0.25%/yr. Oslo and UCI models ran with fixed N_2O burden and, based on a UCI-c29 test case, have their lifetimes increase by 0.4%. Because models have different atmospheric dry-air masses, all burdens are calculated from the lower tropospheric mean N_2O abundance (ppb) using the relationship 4.79 Tg N/ppb [*Prather et al.*, 2012]. For MLS, the average N_2O over the period is taken as 322.2 ppb. MLS-G standard simulation used transient solar activity for the period of MLS observations, while MLS-U used the average of two solar conditions (Solar Ultraviolet Spectral Irradiance Monitor 11 November 1994(low) and 29 March 1992(high)). MLS-G solar maximum conditions are representative, while the MLS-U "solar maximum" simulation is high, but not maximum. The MLS-U lifetime has been corrected for missing 2% of loss below 100 hPa (the lower limit of MLS data). UCI-c29/36 model is a stratosphere-only chemistry model, and its lifetimes are corrected by 1% to account for lack of tropospheric $O(^1D)$ loss. Both c29 results stop in year 2007, but correction is made because the MLS-U lifetime derived for 2005–2007 is almost identical to that over the full period of 2005–2010. Likewise, comparisons of the period 2004/2007 versus period 2004/2010 using cycle 36 and MERRA fields show little difference (±0.9 years). G2d has reduced variability using yearly repeating steady state transport.

with largest differences near the peak loss at 10 hPa. These results are explained for the most part by the lower average tropical abundances of the modeled N_2O between 24 and 40 km, see Figure 2a. Simulated profiles of N_2O are typically lower than MLS values but are within 10%. The difference between two IFS versions are clear in Figure 2: UCI-c29 has more rapid upwelling and higher N_2O below 30 km, whereas UCI-c36 has slower upwelling (or more rapid horizontal dispersion) from 20 to 40 km. The best matches to the MLS N_2O profiles are from GMI, UCI-c29 and Oslo-c29 (not shown). G2d-M (using 2-D monthly mean residual circulation fields derived from the same MERRA fields used directly in GMI) and G2d (using a steady state yearly repeating transport) are similar to UCI-c36, and all have consistently lower N_2O abundances than MLS. A more quantitative comparison of the 10 hPa N_2O abundances is given in Table 2, where the mean and standard deviation of the monthly mean 20°S–20°N abundances are given under "stratospheric N_2O." This statistic emphasizes the core tropics more than in Figure 2, and the spread across models widens. Three models (GMI, UCI-c29, and Oslo-c29) are about 10% below MLS values, and the other models (G2d-M, G2d, UCI-c36, and Oslo-c36) are about 20% below.

MLS observations of N_2O show large-scale, quasi-biennial variability within the tropical upwelling region (20°S–20°N) at the critical altitude of 10 hPa on a monthly zonal-mean basis. These variations are well matched in most models, see Figure 3. As noted before, UCI-c29 (and Oslo-c29, nearly identical and not shown) as well as GMI are similar in magnitude to MLS data but down one contour level (20 ppb), while UCI-c36 (Oslo-c36) and G2d-M are reduced by two or more contour levels. The UCI-c36 N_2O variability is less well correlated with observations than is that of UCI-c29. The G2d and GEOSCCM models are not matched to specific years and not shown. Overall, both the ECMWF and MERRA meteorology produce a modeled 10 hPa N_2O surface that is biased but highly correlated with the MLS observations, indicating that transport variations in the tropical midstratosphere on a month-by-latitude basis are well represented.

The other major controlling factor for N_2O lifetimes is the profile of overhead O_3. Differences in the O_3 profiles (Figure 2b) can help explain why the lifetimes listed in Table 2 are not inversely related to the 10 hPa N_2O abundances. UCI-c29 matches the MLS tropical O_3 profiles with GMI being slightly smaller and UCI-c36 being larger. The greater O_3 in UCI-c36 absorbs more solar ultraviolet, thus reducing the N_2O loss even more than expected from the smaller N_2O abundances. Both GSFC 2-D models (G2d-M and G2d) have nearly identical O_3 profiles that in the 30–40 km region are almost 10% less than MLS. These G2d offsets cancel in terms of

total N_2O loss with more solar ultraviolet enhancing the loss of the reduced levels of N_2O. Thus, both G2d lifetimes are smaller than the GMI lifetime, even though their N_2O abundances are 10–20% smaller.

All models match the monthly seasonality of N_2O loss in MLS-G/U as shown in Figure 4. The Oslo/UCI-c29 results are not so smooth since there are only three overlapping years. Other models show different levels of flattening (or reduction) of the October-November-December month period, but the overall cycles with the February-March peak and June-July trough are in agreement. The greatest difference in Figure 4 is the overall magnitude of the loss, and this large range in modeled N_2O lifetime is summarized in Table 2.

For models using met data back to 1997, we find that the 1997–2010 average lifetime was about 2 years shorter than the 2005–2010 MLS period lifetime, indicating more rapid loss of N_2O in the earlier period. The pre-2005 period thus has a systematically different circulation in the tropical middle stratosphere leading to more rapid upwelling of N_2O, which might be a response to the last solar maximum that occurred during this pre-Aura period or to a change in the observing system used to generate the met data. It cannot be due to photochemical changes driven by the solar cycle since several models did not include this.

The interannual variability in the N_2O lifetime for 1997–2010 is shown in Figure 5. The models using IFS forecast or MERRA-assimilated met data show realistic variations when compared with the MLS-G/U results. The steady state G2d results are shown as a gray bar for the year 2010. In terms of correlations, MLS-G and MLS-U are nearly identical ($R = 0.98$). In terms of model correlations with MLS-G, the G2d-M, Oslo-c29, and UCI-c29 models are excellent (0.85–0.90), but GMI, Oslo-c36, and UCI-c36 models do not match as well (~0.78). It is not clear why the GMI and G2d-M should not be more closely correlated with each other. This may be due to small differences caused in converting the MERRA met fields to 2-D transport (via the heating rates and eddy fluxes) for G2d-M as opposed to using the direct MERRA 3-D wind field in GMI.

A critical part of the stratospheric nitrogen chemistry involves production via reaction (R5) of odd nitrogen ($NO_y = NO + NO_2 + HNO_3 +$ others), which in turn drives catalytic O_3 loss centered about 35 km [*Crutzen*, 1970; *Johnston*, 1971]. For MLS-U, 5.7% of the N_2O loss produces NO_y, and this primary production (Figure 1a) has a lower center of mass than the total N_2O loss because $O(^1D)$ reactions become relatively more important than photolysis in the lower stratosphere. Consequently, the N_2O-NO_y tracer relationship [*Murphy and Fahey*, 1994] is curved in the lower stratosphere. About 30% of primary NO_y produced is lost following photolysis of NO (J_{NO}) in the upper stratosphere and mesosphere [*Olsen et al.*, 2001]. While this photochemical process is included in the CTMs, it cannot be derived simply from the MLS data, and modeling of J_{NO} remains highly uncertain (±30% or more [see *PhotoComp*, 2010]).

Stratospheric NO_y, however, is the key link between N_2O and O_3 chemistries that causes an N_2O perturbation to decay more rapidly than indicated by the atmospheric lifetime [*Prather*, 1998], and thus, we seek an observational test of the modeled NO_y to understand differences in the modeled lifetime sensitivity to burden, $s \equiv \partial \ln(\text{lifetime})/\partial \ln(\text{burden})$, and the resulting lifetime feedback factor, $ff = 1/(1-s)$ (see Table 4.5 of *Prather et al.* [2001]). We focus on the tropics where most N_2O is lost: values of NO_y derived from satellite observations show a broad peak of about 16 ppb near 40 km that varies with season and year and that falls off rapidly at lower altitudes [*Brohede et al.*, 2008; *Jones et al.*, 2011]. As a robust measure of the total amount of stratospheric NO_y, we integrate the 30°S–30°N column of NO_y above 100 hPa (expressed in Dobson unit (DU), 2.687×10^{16} molecules/cm^2) and compare with MIPAS observations (Figure 6). The observations have a mean column of 0.39 DU with a March minimum and July maximum and with a minimum-to-maximum amplitude of ~12%. The models show similar seasonal patterns and fall within ±16% of the MIPAS value. The G2d model is an exception with a very weak seasonal cycle in NO_y columns. Mean columns are summarized in Table 2.

4. N_2O Lifetimes and Chemical Feedback

The N_2O lifetimes from the MLS data and the CTMs are summarized in Table 2. All the models in this study have too little N_2O loss and hence longer lifetimes. Numerous small, percent-level corrections to the lifetimes have been made due to the different chemistries and methods of calculation. Many are noted above and summarized in the table notes. For example, the results here consist of both transient (MLS-G/U, GMI, and G2d-M) and steady state calculations (UCI and Oslo), and the difference between these two

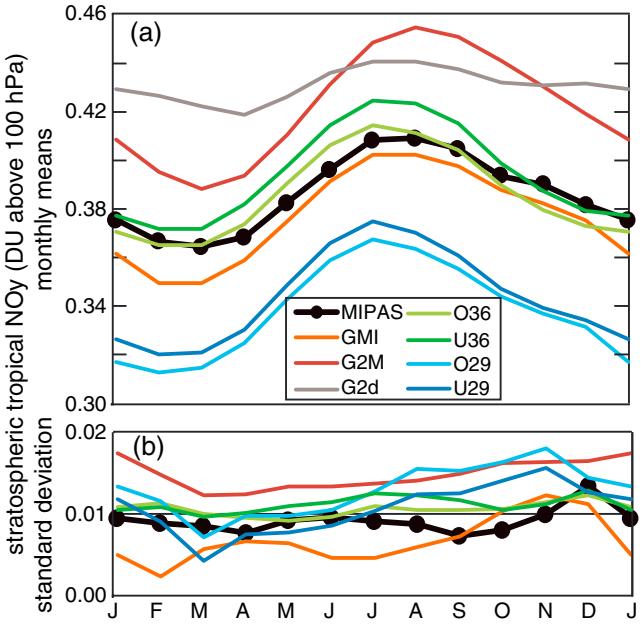

Figure 6. Stratospheric tropical NO_y columns (DU, $P < 100$ hPa, 30°S–30°N) by month showing (a) absolute columns and (b) monthly standard deviations over the MLS period. MIPAS observations (black solid + dots) are compared with models.

approaches has been discussed [*SPARC*, 2013; *WMO*, 2014]. In the transient calculations, the N_2O lower tropospheric abundance increases at the observed rate of about 0.8 ppb/yr (0.25%/yr). Given that the lag for the mixed tropospheric abundance to reach the tropical midstratosphere is a couple of years, the troposphere accumulates an additional burden. In transient versus steady state simulations with UCI-c29, we find that transient lifetimes are about 0.4% larger than steady state ones, and we have so corrected the Oslo and UCI lifetimes in Table 2.

Our semiempirical estimate of the current lifetime, 116 ± 9 years, is based on the MLS-G/U calculations and has a 1 sigma uncertainty of 8%. The only sources of uncertainty here are those in the MLS-measured profiles (N_2O, O_3, and *T*) and those in the photochemical submodels (J_{N2O} and $O(^1D)$). We assume that uncertainties in the O_3 and *T* profiles (affecting the photochemical model uncertainty) are negligible since these measurements have a longer history of satellite measurement and calibration. We identify the primary measurement uncertainty with the N_2O profile in the 30–3 hPa altitude range (N_2O~40–240 ppb). The possible bias in the MLS N_2O measurements near 10 hPa has been assessed as being less than 10% [*Lambert et al.*, 2007], and taking this as a 90% confidence level, we place a generous 1 sigma uncertainty of 7% on the N_2O abundances which translates directly to the N_2O loss. Uncertainty in the photochemical data leads to a 1 sigma uncertainty of 3% in the photochemically modeled lifetime (see Chapter 3 of *SPARC* [2013]). The uncertainty in the N_2O burden is negligible because the mass of the atmosphere is well known and the fall-off of N_2O in the stratosphere is well characterized [*Prather et al.*, 2012]. Combining the two major uncertainties, we get 7.6% and adopt 8% as a symmetric 1 sigma uncertainty in the lifetime. Note that the dominant factor is the N_2O abundance and that adding another 3% uncertainty (e.g., from O_3 and *T*) would not change this value. GEOSCCM is the only model here whose lifetime fits within this uncertainty; Oslo-c29, UCI-c29, and both G2d models lie just above the upper range; and Oslo-c36, UCI-c36, and GMI models have lifetimes more than 2 sigma above. Some but not all of the model range in lifetimes can be attributed to the low N_2O abundances near 10 hPa in the tropics.

Our uncertainty is notably less than previous semiempirical estimates based on the pre-MLS satellite data [*Ko et al.*, 1991; *Minschwaner et al.*, 1998], in part because of the much denser, more accurate set of MLS colocated observations of N_2O, O_3, and T that resolve the quasi-biennial cycle. The separately modeled and satellite-derived N_2O lifetimes updated in *SPARC* [2013] are based on pre-MLS data and have essentially the same lifetime as our best estimate, especially when one considers the large interannual variability (±6 years) not resolved in the pre-MLS data (see Figure 5). The Stratospheric Processes and their Role in Climate (SPARC) overall best estimate, based on models, satellite data, and tracer-tracer lifetimes, is slightly higher with greater uncertainty, 123 years (range of 104–152 years), because of the inclusion of a 144 year lifetime determined from tracer-tracer correlations. Tracer-tracer correlations in the lower stratosphere are used to derive relative lifetimes [*Volk et al.*, 1997; *Brown et al.*, 2013; *Laube et al.*, 2013], but this approach is not useful here because the uncertainties are much larger (e.g., they propagate from the reference gas lifetime, and even modeled two gas tracer correlations like N_2O-$CFCl_3$ are difficult to interpret as a single slope [*Avallone and Prather*, 1997]).

Table 3. Preindustrial (PI) N_2O Lifetime Changes (Approximately %) Separated by Key Factors, Shown as ln [Lifetime(PI)/Lifetime(Present Day)][a]

Model	PI From N_2O Change	PI From ODS Change	Full PI
G2d	+0.018	+0.048	+0.077[b]
Oslo-c29	+0.010	+0.033	+0.043
UCI-c29	+0.012	+0.029	+0.039

[a]Note that PI changes include N_2O dropping from 321 ppb (2004–2010) to 270 ppb, anthropogenic ozone-depleting substances (ODS) dropping to zero, CH_4 dropping from 1785 ppb to 722 ppb, and climate change driven by CO_2 dropping from 384 ppm to 278 ppm. Individual models chose slightly, but insignificantly different ranges for the PI, and the values from *IPCC* [2013b] are quoted here.
[b]G2d has a stratospheric circulation that responds dynamically to heating changes from O_3 and CO_2 (in Full PI); see *Fleming et al.* [2011].

Our estimate of the lifetime sensitivity of N_2O to its burden is $s = -0.065 \pm 0.010$, where the ±0.010 is a 1 sigma uncertainty as it includes almost the entire range of models except for G2d. Thus, the feedback factor is $ff = 0.94 \pm 0.01$, and the effective residence time of an N_2O perturbation is 109 ± 10 years [e.g., *Prather*, 2007; *Prather and Holmes*, 2013]. Unfortunately, there is no semiempirical method to derive this sensitivity using MLS observations, but given the limited range for this value since first reported in 1998, we feel that ±15% 1 sigma uncertainty is a conservative choice. All chemistry-transport models here are consistent with this range, except for G2d, whose sensitivity is nearly twice as large (Table 2). Both G2d and G2d-M have identical chemistries and similar N_2O lifetimes and tropical NO_y columns but very different sensitivities. Analysis shows that with a greater burden of N_2O, G2d's interactive circulation is responding as slightly reduced O_3 (−2%), heating rates, and temperatures (−0.3 K); enhanced upwelling with age of air changed by −0.05 years; and consequently more N_2O loss. While the free-running GEOSCCM shows similar reductions in O_3 and temperature, it does not simulate a circulation enhancement. At this time we do not include the −0.11 feedback factor in G2d in our uncertainty range but must recognize it as presenting an open question.

There is also no simple relationship found in Table 2 between the lifetime sensitivity and the NO_y column, in contrast to what was expected. An interesting finding from the 14 year UCI-c36 calculation was that the lifetime sensitivity took more than 7 years to stabilize following a sudden 10% increase at the lower boundary, even though the lifetime appeared to stabilize more rapidly. Surprisingly, our best estimates of lifetime and feedback factor have not changed much since the first multimodel estimates were made in 2001 (see Table 4.5 of *Prather et al.* [2001]).

Analysis of the preindustrial (PI) lifetime of N_2O was made with G2d, Oslo-c29, and UCI-c29, with results shown in Table 3. The PI simulations assumed N_2O tropospheric abundance of 270 ppb (versus 321 ppb), CH_4 abundance of 722 ppb (versus 1785 ppb), CO_2 abundance of 278 ppm (versus 384 ppm, used in G2d only), and zero anthropogenic ozone-depleting substances (ODSs) [*IPCC*, 2013b]. Changes in lifetime, calculated as the natural log of PI lifetime divided by present-day lifetime, are estimated at +1 to +2% due to the lower levels of N_2O alone. The other major change, a +3 to +5% increase due to the lack of anthropogenic ODS, is caused by the higher levels of PI 40–50 km tropical O_3, leading to reduced penetration of solar radiation to 32 km, and hence reduced losses of N_2O. The full PI lifetime is estimated from these three models to be +4% to +8% larger than present day, with the upper range including CO_2 dynamical effects (G2d only). We adopt +6%, to give a lifetime of 123 years. As long as the uncertainty in this change (±2%) is independent of other errors, then the 1 sigma range remains at about ±8%.

5. An Overview of Lifetimes, Budgets, and Uncertainties

This study has rigorously tested four global chemistry-transport models' ability to simulate the observed distribution and loss patterns of N_2O based on 5 years of MLS observations. These tests address seasonal and interannual variability showing that the models have high fidelity in reproducing the measurements on a month-by-month basis in spite of having lifetimes that are biased high by 9% to 26%, outside of the ±8% uncertainty range. Most biases can be understood in terms of lower model N_2O abundances in the middle stratosphere or (in some cases) O_3 profiles that are notably different from MLS data. The GEOSCCM, a free-running climate model not expected to reproduce the observed variations in N_2O lifetime (e.g.,

Figure 5), was added to check if the N_2O lifetime sensitivity was significantly perturbed by induced circulation changes. It was not. GEOSCCM has the most accurate simulation of multiyear average N_2O abundances in the middle tropical stratosphere among all the models here, and it has a lifetime within the uncertainty range of the MLS-derived value. Overall, this points to the importance of circulation and net tracer transport in the middle tropical stratosphere in determining N_2O lifetime.

What is the best estimate for the current N_2O lifetime, one that includes the steady slow increase (0.25%/yr) in burden? The SPARC assessment's recommendation (see Table 6.1 of *SPARC* [2013]) is 123 years with a 1 sigma range of 113 to 148 years based on a range of models, observations, and tracer correlations. Our 1 sigma range of 109 to 125 years overlaps with but is limited to the lower half of the SPARC range. *Chipperfield et al.* [2014]; also Chapter 5 from SPARC] averaged the results from six chemistry-climate models to estimate a steady state lifetime of 115 years with a model variance of 8%. To correct this to current observations (the transient as recorded in MLS data) would add about 0.5 years, and thus, this result is essentially identical to the semiempirical MLS lifetime derived here. What is unusual is that the models in this study (CCM and CTMs) calculate much longer lifetimes, 120 to 146 years, almost outside the range of the SPARC models, 105 to 127 years. GEOSCCM participated in both studies (120 years in this study versus 117 years in SPARC) as did G2d (130 years versus 125 years). The differences are not greatly significant and may depend on the scaling of tropospheric abundance (ppb) to burden (Tg N), but both models are at the high end of the SPARC models and the low end of the models here. Thus, the small variance of the SPARC models may not be representative. GEOSCCM used here and in SPARC is closely related in terms of chemistry to GMI but has very different lifetimes, 120 versus 137 years. The primary difference for this split lies with the meteorology. The MERRA fields are known to have excessive subtropical mixing in the lower stratosphere, which reduces N_2O in the tropics, thus reducing its flux to the tropical midstratosphere. Similarly, the IFS fields for cycle 36 appear to have more stagnant vertical transport in the midstratosphere than cycle 29. The N_2O lifetime is a good diagnostic of the circulation and mixing below the middle stratosphere [*Strahan et al.*, 2011].

How does this new lifetime change our estimates of N_2O emissions, both preindustrial and present-day anthropogenic? The evaluation of emissions based on observed abundances and lifetime (both PI and present) gave PI emissions of 9.1 ± 1.0 Tg N/yr and present anthropogenic emissions of 6.5 ± 1.3 Tg N/yr (assuming that PI emissions, but not lifetime, remain constant) [*Prather et al.*, 2012]. Those values were based on the then-most-recent model study with a lifetime of 131 years [*Fleming et al.*, 2011]. Correcting to our current lifetime recommendation increases the PI natural sources to 10.5 Tg N/yr but hardly changes the anthropogenic source, 6.6 Tg N/yr. Uncertainties do not significantly change.

How will the N_2O lifetime change in the future? The SPARC model's year 2100 simulations showed a wide range of changes in lifetime from −6 years to +6 years [*Chipperfield et al.*, 2014]. If a ±5% uncertainty in the future lifetime was a true bound, then the climate and ozone impacts of future N_2O emissions can be evaluated with some confidence. However, the seemingly random shifts in future lifetime need to be evaluated in terms of the key factors driving them, as was attempted for the PI lifetime in Table 3 here. *Douglass et al.* [2014] were able to identify the primary factors causing the wide range of future ozone projections in CCMs by separating their responses to increasing greenhouse gases from their temperature and chemistry responses to decreasing ODSs. If the goal is to understand future changes in the lifetimes of gases controlled by stratospheric chemistry, then a more rigorous protocol of model studies is needed to assess separately, e.g., the decline in ODS, future stratospheric temperatures, and the role of changes in transport.

Acknowledgments

Tabulated data sets used in the figures here will be posted at ftp://halo.ess.uci.edu or are otherwise available from the corresponding author (mprather@uci.edu). Research at UCI was supported by NASA grants NNX09AJ47G and NNX13AL12G and DOE awards DE-SC0007021 and DE-SC0012536. N.M.D. was supported by UCI NSF REU 1005042. The GEOSCCM contribution was supported by the NASA MAP program. B.F. was supported by the Spanish MCINN under grant AYA2011-23552 and EC FEDER funds. Work at the Jet Propulsion Laboratory was performed under contract with NASA. The assistance of Ryan Fuller (at JPL) for the creation of MLS data sets used here is acknowledged. The GSFC 2-D model contribution was supported by the NASA Atmospheric Composition: Modeling and Analysis Program.

References

Avallone, L. M., and M. J. Prather (1997), Tracer-tracer correlations: Three-dimensional model simulations and comparisons to observations, *J. Geophys. Res.*, *102*(D15), 19,233–19,246, doi:10.1029/97JD01123.

Bian, H. S., and M. J. Prather (2002), Fast-J2: Accurate simulation of stratospheric photolysis in global chemical models, *J. Atmos. Chem.*, *41*(3), 281–296.

Brohede, S., C. A. McLinden, J. Urban, C. S. Haley, A. I. Jonsson, and D. Murtagh (2008), Odin stratospheric proxy NO_y measurements and climatology, *Atmos. Chem. Phys.*, *8*(19), 5731–5754.

Brown, A. T., C. M. Volk, M. R. Schoeberl, C. D. Boone, and P. F. Bernath (2013), Stratospheric lifetimes of CFC-12, CCl_4, CH_4, CH_3Cl and N_2O from measurements made by the Atmospheric Chemistry Experiment-Fourier Transform Spectrometer (ACE-FTS), *Atmos. Chem. Phys.*, *13*(14), 6921–6950, doi:10.5194/acp-13-6921-2013.

Chipperfield, M. P., et al. (2014), Multimodel estimates of atmospheric lifetimes of long-lived ozone-depleting substances: Present and future, *J. Geophys. Res. Atmos.*, *119*, 2555–2573, doi:10.1002/2013JD021097.

Ciais, P., et al. (2013), Carbon and other biogeochemical cycles, in *Climate Change 2013: The Physical Science Basis. Contribution of Working Group I to the Fifth Assessment Report of the Intergovernmental Panel on Climate Change*, edited by T. F. Stocker et al., pp. 465–570, Cambridge Univ. Press, Cambridge, U. K.

Crutzen, P. J. (1970), Influence of nitrogen oxides on atmospheric ozone content, *Q. J. R. Meteorol. Soc.*, *96*(408), 320–325.

Douglass, A. R., R. S. Stolarski, S. E. Strahan, and P. S. Connell (2004), Radicals and reservoirs in the GMI chemistry and transport model: Comparison to measurements, *J. Geophys. Res.*, *109*, D16302, doi:10.1029/2004JD004632.

Douglass, A. R., S. E. Strahan, L. D. Oman, and R. S. Stolarski (2014), Understanding differences in chemistry climate model projections of stratospheric ozone, *J. Geophys. Res. Atmos.*, *119*, 4922–4939, doi:10.1002/2013JD021159.

Erisman, J. W., J. N. Galloway, S. Seitzinger, A. Bleeker, N. B. Dise, A. M. R. Petrescu, A. M. Leach, and W. de Vries (2013), Consequences of human modification of the global nitrogen cycle, *Philos. Trans. R. Soc. B*, *368*, 1621, doi:10.1098/rstb.2013.0116.

Fleming, E. L., C. H. Jackman, R. S. Stolarski, and A. R. Douglass (2011), A model study of the impact of source gas changes on the stratosphere for 1850–2100, *Atmos. Chem. Phys.*, *11*(16), 8515–8541, doi:10.5194/acp-11-8515-2011.

Froidevaux, L., et al. (2008), Validation of Aura Microwave Limb Sounder stratospheric ozone measurements, *J. Geophys. Res.*, *113*, D15S20, doi:10.1029/2007JD008771.

Froidevaux, L., et al. (2015), Global OZone Chemistry And Related Datasets for the Stratosphere (GOZCARDS): Methodology and sample results with a focus on HCl, H_2O, and O_3, *Atmos. Chem. Phys. Discuss.*, *15*, 5849–5957, doi:10.5194/acpd-15-5849-2015.

Funke, B., M. Lopez-Puertas, G. P. Stiller, and T. von Clarmann (2014), Mesospheric and stratospheric NO_y produced by energetic particle precipitation during 2002–2012, *J. Geophys. Res. Atmos.*, *119*, 4429–4446, doi:10.1002/2014JD022423.

Galloway, J. N., A. R. Townsend, J. W. Erisman, M. Bekunda, Z. Cai, J. R. Freney, L. A. Martinelli, S. P. Seitzinger, and M. A. Sutton (2008), Transformation of the nitrogen cycle: Recent trends, questions, and potential solutions, *Science*, *320*(5878), 889–892, doi:10.1126/science.1136674.

Hsu, J., and M. J. Prather (2010), Global long-lived chemical modes excited in a 3-D chemistry transport model: Stratospheric N_2O, NO_y, O_3 and CH_4 chemistry, *Geophys. Res. Lett.*, *37*, L07805, doi:10.1029/2009GL042243.

Intergovernmental Panel on Climate Change (IPCC) (2007), *Climate Change 2007: The Physical Science Basis. Contribution of Working Group I to the Fourth Assessment Report of the Intergovernmental Panel on Climate Change*, pp. 996, Cambridge Univ. Press, Cambridge, U. K.

Intergovernmental Panel on Climate Change (IPCC) (2013a), *Climate Change 2013: The Physical Science Basis, the IPCC WGI Contribution to the Fifth Assessment Report, Report of the Intergovernmental Panel on Climate Change*, edited by T. F. Stocker et al., pp. 999, Cambridge Univ. Press, Cambridge, U. K.

Intergovernmental Panel on Climate Change (IPCC) (2013b), Annex II: Climate system scenario tables, in *Climate Change 2013: The Physical Science Basis. Contribution of Working Group I to the Fifth Assessment Report of the Intergovernmental Panel on Climate Change*, edited by T. F. Stocker et al., pp. 1395–1446, Cambridge Univ. Press, Cambridge, U. K.

Jackman, C. H., C. E. Randall, V. L. Harvey, S. Wang, E. L. Fleming, M. Lopez-Puertas, B. Funke, and P. F. Bernath (2014), Middle atmospheric changes caused by the January and March 2012 solar proton events, *Atmos. Chem. Phys.*, *14*(2), 1025–1038, doi:10.5194/acp-14-1025-2014.

Johnston, H. (1971), Reduction of stratospheric ozone by nitrogen oxide catalysts from supersonic transport exhaust, *Science*, *173*, 517–522.

Jones, A., G. Qin, K. Strong, K. A. Walker, C. A. McLinden, M. Toohey, T. Kerzenmacher, P. F. Bernath, and C. D. Boone (2011), A global inventory of stratospheric NO_y from ACE-FTS, *J. Geophys. Res.*, *116*, D17304, doi:10.1029/2010JD015465.

Kirtman, B., et al. (2013), Near-term climate change: Projections and predictability, in *Climate Change 2013: The Physical Science Basis, IPCC WGI Contribution to the Fifth Assessment Report*, edited by T. F. Stocker et. al., pp. 953–1028, Cambridge Univ. Press, Cambridge, U. K.

Ko, M. K. W., N. D. Sze, and D. K. Weisenstein (1991), Use of satellite data to constrain the model-calculated atmospheric lifetime for N_2O: Implications for other trace gases, *J. Geophys. Res.*, *96*(D4), 7547–7552, doi:10.1029/91JD00273.

Lambert, A., et al. (2007), Validation of the Aura Microwave Limb Sounder middle atmosphere water vapor and nitrous oxide measurements, *J. Geophys. Res.*, *112*, D24S36, doi:10.1029/2007JD008724.

Laube, J. C., A. Keil, H. Bonisch, A. Engel, T. Rockmann, C. M. Volk, and W. T. Sturges (2013), Observation-based assessment of stratospheric fractional release, lifetimes, and ozone depletion potentials of ten important source gases, *Atmos. Chem. Phys.*, *13*(5), 2779–2791, doi:10.5194/acp-13-2779-2013.

Li, F., D. W. Waugh, A. R. Douglass, P. A. Newman, S. Pawson, R. S. Stolarski, S. E. Strahan, and J. E. Nielsen (2012), Seasonal variations of stratospheric age spectra in the Goddard Earth Observing System Chemistry Climate Model (GEOSCCM), *J. Geophys. Res.*, *117*, D05134, doi:10.1029/2011JD016877.

Livesey, N. J., et al. (2011), EOS MLS version 3.3 level 2 data quality and description document, Tech. Rep., Jet Propulsion Laboratory. [Available at http://mls.jpl.nasa.gov/.]

Meinshausen, M., et al. (2011), The RCP greenhouse gas concentrations and their extensions from 1765 to 2300, *Clim. Change*, *109*(1–2), 213–241, doi:10.1007/s10584-011-0156-z.

Minschwaner, K., R. W. Carver, B. P. Briegleb, and A. E. Roche (1998), Infrared radiative forcing and atmospheric lifetimes of trace species based on observations from UARS, *J. Geophys. Res.*, *103*(D18), 23,243–23,253, doi:10.1029/98JD02116.

Minschwaner, K., L. Hoffmann, A. Brown, M. Riese, R. Muller, and P. F. Bernath (2013), Stratospheric loss and atmospheric lifetimes of CFC-11 and CFC-12 derived from satellite observations, *Atmos. Chem. Phys.*, *13*(8), 4253–4263, doi:10.5194/acp-13-4253-2013.

Murphy, D. M., and D. W. Fahey (1994), An estimate of the flux of stratospheric reactive nitrogen and ozone into the troposphere, *J. Geophys. Res.*, *99*(D3), 5325–5332, doi:10.1029/93JD03558.

Myhre, G., et al. (2013), Anthropogenic and natural radiative forcing, in *Climate Change 2013: The Physical Science Basis, IPCC WGI Contribution to the Fifth Assessment Report*, edited by T. F. Stocker et al., pp. 659–740, Cambridge Univ. Press, Cambridge, U. K.

Olsen, S. C., C. A. McLinden, and M. J. Prather (2001), Stratospheric N_2O-NO_y system: Testing uncertainties in a three-dimensional framework, *J. Geophys. Res.*, *106*(D22), 28,771–28,784, doi:10.1029/2001JD000559.

Olson, J., et al. (1997), Results from the Intergovernmental Panel on Climatic Change Photochemical Model Intercomparison (PhotoComp), *J. Geophys. Res.*, *102*(D5), 5979–5991, doi:10.1029/96JD03380.

Oman, L. D., and A. R. Douglass (2014), Improvements in total column ozone in GEOSCCM and comparisons with a new ozone-depleting substances scenario, *J. Geophys. Res. Atmos.*, *119*, 5613–5624, doi:10.1002/2014JD021590.

Pesnell, W. D. (2014), Predicting solar cycle 24 using a geomagnetic precursor pair, *Sol. Phys.*, *289*(6), 2317–2331, doi:10.1007/s11207-013-0470-x.

PhotoComp (2010), Chapter 6: Stratospheric chemistry, in *SPARC Rep. 5, The Evaluation of Chemistry-Climate Models*, *WCRP-132, WMO/TD-No. 1526*, edited by V. Erying, T. Shepherd, and D. Waugh, pp. 194–202, World Clim. Res. Programme, Geneva, Switzerland.

Prather, M., et al. (2001), Chapter 4: Atmospheric chemistry and greenhouse gases, in *Climate Change 2001: The Scientific Basis. Third Assessment Report of the Intergovernmental Panel on Climate Change*, pp. 239–287, Cambridge Univ. Press, Cambridge, U. K.

Prather, M. J. (1998), Time scales in atmospheric chemistry: Coupled perturbations to N_2O, NO_y, and O_3, *Science*, *279*(5355), 1339–1341.

Prather, M. J. (2007), Lifetimes and time scales in atmospheric chemistry, *Phil. Trans. R. Soc. A*, *365*(1856), 1705–1726, doi:10.1098/rsta.2007.2040.

Prather, M. J., and C. D. Holmes (2013), A perspective on time: Loss frequencies, time scales and lifetimes, *Environ. Chem.*, *10*(2), 73–79.

Prather, M. J., and J. Hsu (2010), Coupling of nitrous oxide and methane by global atmospheric chemistry, *Science*, *330*, 952–954, doi:10.1126/science.1196285.

Prather, M. J., et al. (2009), Tracking uncertainties in the causal chain from human activities to climate, *Geophys. Res. Lett.*, *36*, L05707, doi:10.1029/2008GL036474.

Prather, M. J., C. D. Holmes, and J. Hsu (2012), Reactive greenhouse gas scenarios: Systematic exploration of uncertainties and the role of atmospheric chemistry, *Geophys. Res. Lett.*, *39*, L09803, doi:10.1029/2012GL051440.

Sander, S. P., et al. (2011), Chemical kinetics and photochemical data for use in atmospheric studies *Eval. No. 17*, Jet Propulsion Laboratory, Pasadena, Calif.

Schwartz, M. J., et al. (2008), Validation of the Aura Microwave Limb Sounder temperature and geopotential height measurements, *J. Geophys. Res.*, *113*, D15S11, doi:10.1029/2007JD008783.

Søvde, O. A., M. J. Prather, I. S. A. Isaksen, T. K. Berntsen, F. Stordal, X. Zhu, C. D. Holmes, and J. Hsu (2012), The chemical transport model Oslo CTM3, *Geosci Model Dev*, *5*(6), 1441–1469, doi:10.5194/gmd-5-1441-2012.

SPARC (2013), SPARC report on lifetimes of stratospheric ozone-depleting substances, their replacements, and related species, in *SPARC Rep. 6, WCRP-15/2013*, edited by M. K. W. Ko et al., World Clim. Res. Programme, Geneva, Switzerland.

Strahan, S. E., et al. (2011), Using transport diagnostics to understand chemistry climate model ozone simulations, *J. Geophys. Res.*, *116*, D17302, doi:10.1029/2010JD015360.

Strahan, S. E., A. R. Douglass, and P. A. Newman (2013), The contributions of chemistry and transport to low arctic ozone in March 2011 derived from Aura MLS observations, *J. Geophys. Res. Atmos.*, *118*, 1563–1576, doi:10.1002/jgrd.50181.

Thompson, R. L., et al. (2014), TransCom N_2O model inter-comparison—Part 1: Assessing the influence of transport and surface fluxes on tropospheric N_2O variability, *Atmos. Chem. Phys.*, *14*(8), 4349–4368, doi:10.5194/acp-14-4349-2014.

Volk, C. M., J. W. Elkins, D. W. Fahey, G. S. Dutton, J. M. Gilligan, M. Loewenstein, J. R. Podolske, K. R. Chan, and M. R. Gunson (1997), Evaluation of source gas lifetimes from stratospheric observations, *J. Geophys. Res.*, *102*(D21), 25,543–25,564, doi:10.1029/97JD02215.

World Meteorological Organization (WMO) (2011), *Scientific Assessment of Ozone Depletion: 2010 Global Ozone Research and Monitoring Poject–Rep. 50*, World Meteorol. Organ., Geneva, Switzerland.

World Meteorological Organization (WMO) (2014), *Scientific Assessment of Ozone Depletion: 2014 Global Ozone Research and Monitoring Poject–Rep. 56*, World Meteorol. Organ., Geneva, Switzerland.